EuroIntervention

In vivo evaluation of stent strut distribution patterns in the bioabsorbable everolimus-eluting device: an OCT *ad hoc* analysis of the revision 1.0 and revision 1.1 stent design in the ABSORB clinical trial

Takayuki Okamura[1], MD, PhD; Scot Garg[1], MBChB, MRCP; Juan Luis Gutiérrez-Chico[1], MD, PhD; Eun-Seok Shin[1], MD, PhD; Yoshinobu Onuma[1], MD; Héctor M. García-García[1,2], MD, PhD; Richard J. Rapoza[3], PhD; Krishnankutty Sudhir[3], MD, PhD; Evelyn Regar[1], MD, PhD; Patrick W. Serruys[1*], MD, PhD

1. Thoraxcenter, Erasmus MC, Rotterdam, The Netherlands; 2. Cardialysis BV, Rotterdam, The Netherlands; 3. Abbott Vascular, Santa Clara, CA, USA

Conflict of interest statement: All authors have approved the final manuscript, which has not been published and is not under consideration elsewhere. RR and KS are employees of Abbott Vascular. The other authors have no conflict of interest to declare.

KEYWORDS
Stent designs, drug eluting stent, bioabsorbable, strut

Abstract

Aims: The ABSORB Cohort A clinical study has shown the feasibility and safety of the fully bioabsorbable everolimus-eluting structure (BVS, revision 1.0). However, the study also demonstrated somewhat higher acute and late recoil with the BVS structure compared to metallic drug eluting stents. Based on these clinical observations, modifications to the stent design (BVS, revision 1.1) were introduced for the ABSORB Cohort B study in order to decrease recoil. The aim was to compare *in vivo* the strut distribution between the BVS revision 1.0 (Cohort A), and BVS revision 1.1 (Cohort B) designs.

Methods and results: OCT analysis was performed by two independent analysts in four patients from each cohort of the ABSORB study. Strut distribution was assessed in cross-section, and longitudinally in a frame-by-frame analysis. Variables recorded included inter-strut angle, maximum inter-strut angle and number of frames with ≤3 struts. The inter-observer correlation coefficient was also assessed. For both designs, on a patient level there was no significant difference in the number of analysed struts corrected for the length of the scaffold (p=0.78). Likewise, on a frame by frame analysis mean stent area, number of struts per frame, mean maximum inter-strut angle, and mean inter-strut angle were similar for both groups. However, in both structures there was a cyclical variation in the maximum number of struts per frame. The frequency of this variation was significantly higher in Cohort B. The inter-observer correlation coefficient for strut counts, inter-strut angle and maximum inter-strut angle was 0.91, 0.87 and 0.74 respectively.

Conclusions: This *ad hoc* analysis confirms that the revision 1.1 BVS design has a different longitudinal strut distribution to the revision 1.0 BVS design, indicating that the new design has a reduced maximum circular unsupported cross sectional area.

** Corresponding author: Thoraxcenter, Bd583a, Dr.Molewaterplein 40, 3015, GD, Rotterdam, The Netherlands*
E-mail: p.w.j.c.serruys@erasmusmc.nl

Introduction

The ABSORB clinical trial (Cohort A) was a 30 patient first-in-man evaluation of the revision 1.0 bioabsorbable vascular solution (BVS) everolimus eluting stent (Abbott Vascular, Santa Clara, CA, USA).[1] This open-label prospective multi-centre study demonstrated the feasibility of implanting the BVS device, and showed a low rate of major adverse cardiac events at two years follow-up. Furthermore multi-modality imaging confirmed that the scaffold was absorbed within two years.[2]

Despite the impressive clinical outcomes, that were comparable with the XIENCE V® everolimus eluting stent (Abbott Vascular, Santa Clara, CA, USA), the BVS device had a slightly higher, but non-significant acute and late recoil as assessed by baseline quantitative coronary angiography,[3] and six month intravascular ultrasound (IVUS) respectively.[4] Results suggested that this late recoil may be related to the underlying lesion morphology,[4] but more importantly IVUS also suggested a trend for more recoil when fewer struts were present. Recoil was measured at 0.67 (SD 2.04) mm², 0.65 (1.67) mm², and 0.51 (1.64) mm² in three regions scaffolded by three, four to eight, and nine struts respectively (p=not significant).[1] These observations prompted design modifications in order to reduce the maximum circular unsupported cross sectional area (MCUSA), increase radial force, and prolong the time for which the implant scaffolds the vessel, without changing the implant's total absorption time. These design modifications have been incorporated into the revision 1.1 BVS design, which is currently being evaluated in the ABSORB Cohort B study.[5]

Strut distribution is used as a surrogate of the MCUSA because at present there is no established method available to calculate the MCUSA directly. This is primarily because of the inability of conventional intravascular ultrasound (IVUS) and optical coherence tomography (OCT) to produce a spatial arrangement of the strut distribution both in cross section and longitudinally. The purpose of this study was therefore to evaluate the difference in the strut distribution between the two versions of the BVS device using *in vivo* OCT.

Methods

Study design

The study design for the prospective, open label cohort A ABSORB trial has been published elsewhere.[1] In brief, this was a single arm study that enrolled 30 patients at four participating sites between March and July 2006. The larger multicentre Cohort B study which will enrol 80 patients started recruitment in March 2009. In both cohorts patients over the age of 18 years, who had either stable or unstable angina pectoris, or silent ischaemia were suitable for inclusion. All treated lesions were single *de novo* lesions in a native coronary artery with a maximum diameter of 3.0 mm, and a length of ≤8 mm for the 12 mm stent or ≤14 mm for the 18 mm stent, with a percentage diameter stenosis ≥50% and <100%, and a thrombolysis in myocardial infarction (TIMI) flow grade of ≥1. Major exclusion criteria for both studies were patients presenting with an acute myocardial infarction, unstable arrhythmias or patients who had a left ventricular ejection fraction <30%, restenotic lesions, lesions located in the left main coronary artery, lesions involving a side branch >2 mm in diameter, and the presence of thrombus or another clinically significant stenosis in the target vessel. The studies were approved by the ethics committee at each participating institution and each patient gave written informed consent before inclusion.

Study population

The study population comprised of eight patients in total. OCT was not mandated in the ABSORB study, and therefore OCT images were only available for 13 Cohort A patients, of which four were randomly selected for this study, together with the first four patients enrolled in Cohort B (Figure 1).

Study device

Cohort A: The BVS revision 1.0 design was used in ABSORB Cohort A. The implant has a polymer backbone of Poly-L (racemic)-lactic Acid (PLLA) coated with a thin layer of a 1:1 mixture of an amorphous matrix of Poly-D,L (racemic)-lactic acid (PDLLA) polymer, and 100 micrograms/cm² of the anti-proliferative drug everolimus. The implant is radiolucent, but has two platinum markers at each end that allow easy visualisation on angiography and with other imaging modalities. Everolimus suppresses neointimal hyperplasia by blocking growth-factor-derived cell proliferation to arrest the cell cycle in the G1–S phase. The PDLLA allows controlled release of the everolimus such that 80% has eluded by 30-days; the elution rate, tissue concentration and the dose density of everolimus are similar for the BVS device and the XIENCE V® everolimus eluting stent (EES). Both PLLA and PDLLA are fully absorbable. The polymer degrades via a bulk erosion process through hydrolysis of the ester bonds in the backbone. The resulting lactic acid oligomers eventually leave the polymer matrix and are metabolised in surrounding tissues and blood into the pyruvate and Kreb's energy cycles. The time for complete

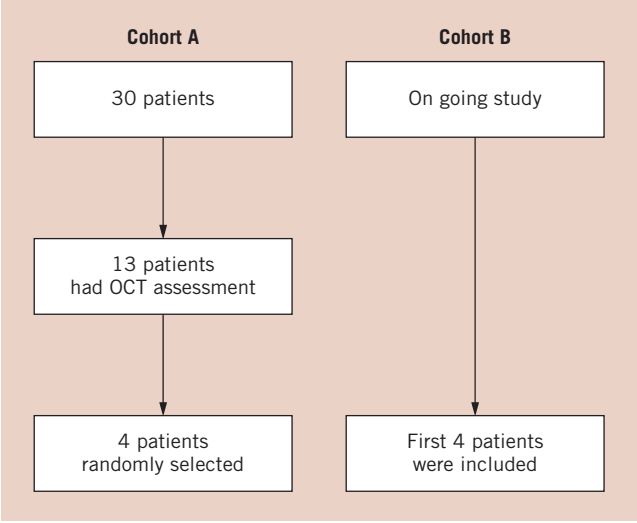

Figure 1. Flow-chart of patient selection.

absorption of the polymer backbone is predicted from preclinical studies to be about two years whereas the polymer coating is absorbed in a faster timeframe.

Physically the scaffold has struts with a thickness of 150 µm, a crossing profile 1.2 mm, and consists of circumferential out-of-phase zigzag hoops linked together by three longitudinal struts between each hoop. Furthermore it needs to be stored at -20°C to prevent creep, physically aging of the polymer and ensure device stability (Figure 2).

Cohort B: The BVS revision 1.1 design is being used in the ABSORB Cohort B study. It uses the same polymers in both the scaffold and coating as the original 1.0 design, and has the same radiolucent platinum markers. Through process refinements, the polymer scaffold is able to provide radial support for longer, whilst retaining the same total time for complete absorption of two years. The strut thickness remains the same; however, the new design has in-phase zigzag hoops linked by bridges. These design changes allow a more uniform strut distribution, which reduces MCUSA and provides greater/more uniform vessel wall support and drug transfer (Figure 2). Implant security has increased, such that dislodgement is unlikely, and the device can now be stored at room temperature.

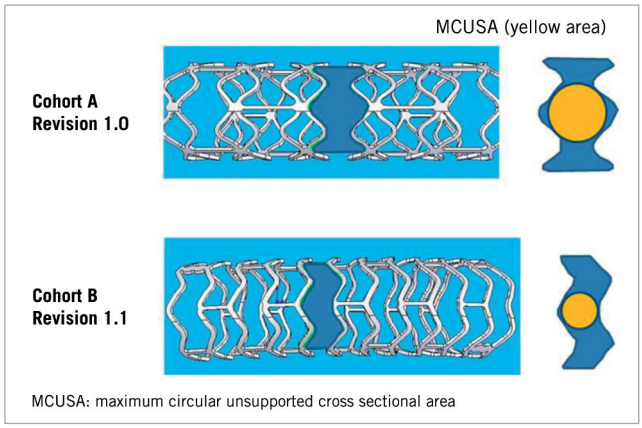

Figure 2. The diagram indicates the different maximum circular unsupported cross sectional areas in both structures.

Imaging procedure

OCT imaging

Cohort A (Table 1): A commercially available OCT system (M2 system, LightLab Imaging Inc, Westford, MA, USA) was used in a Cohort A. This technique, with the use of an infrared light source, has a resolution of 15 µm which is about ten times higher than that of IVUS and therefore allows visualisation of intracoronary structures in great detail. The light source is a 1310 nm broadband super luminescent diode with an imaging depth of about 1.5 mm, an axial resolution of 15 µm, and a lateral resolution of 25 µm. The imaging probe (ImageWire; LightLab Imaging Inc., Westford, MA, USA) has a maximum outer diameter of 0.4826 mm, (0.019") and contains a 0.1524 mm (0.006") fibre-optic imaging core and a distal radio-opaque spring tip, which is similar to conventional guide wires. An OCT catheter (Helios proximal occlusion catheter) is initially advanced distal to the area of interest over a conventional coronary guide wire, which is then replaced with the OCT imaging wire (ImageWire). The OCT catheter is then manually withdrawn proximal to the treated segment, the balloon is inflated at low pressure, crystalloids are used to clear the blood, and the wire containing the imaging core is withdrawn at 1 mm per second. During image acquisition, coronary blood flow is replaced by continuous flushing of Ringer's lactate at 0.5–1.0 mL per second with a power injector (Mark V ProVis; Medrad Inc., Indianola, PA, USA). The highly compliant occlusion balloon remains inflated proximal to the lesion at 0.5 atm (50.66 kPa) or 0.7 atm (70.93 kPa) for a maximum of 30 seconds. Cross-sectional images were acquired at 8.2, and 15.6 frames per second. Cohort B (Table 1): a second generation OCT system (C7XR system; LightLab Imaging Inc, Westford, MA, USA) was used. The underlying principles of OCT imaging remain the same as described above. This system uses a scanning laser which sweeps over a range of wavelength between 1250 and 1350 nm as light source. The 2.7 Fr OCT imaging catheter (Dragonfly; LightLab Imaging Inc, Westford, MA, USA) has a short monorail design, and contains the fibretic core that rotates within a translucent sheath. In Cohort B, the OCT imaging catheter was advanced distal to the region of interest over a 0.014-inch conventional angioplasty guidewire. The pullback was performed during a continuous injection of 3ml/second of X-ray contrast (Iodixanol 370, Visipaque®; GE Healthcare, Cork, Ireland) injected at a maximum pressure of 300 psi through the guiding catheter using an injection pump. Images were acquired at 100 frames per second at an automated pullback speed of 20 mm per second.

OCT analysis

A two-dimensional assessment of distribution of struts was made by measuring the strut distribution using individual OCT frames (i.e., cross-sections). Considering the two scaffold designs, the minimum number of struts that could be present within one frame was three, therefore it follows that the maximum theoretical inter-strut angle expected was 120° (Figure 3). In our experience the minimum number of struts that was observed was two as a consequence of OCT catheter eccentricity, out of field of view (M2

Table 1. A comparison of the different properties of the two OCT systems used in this study.

	OCT system	Frame rate	Pullback speed	Frame thickness	Method of blood removal
Cohort A	LLI M2	8.2 fps (n=2) 15.6 fps (n=2)	1.0 mm/s	0.125 mm 0.0625 mm	Proximal balloon occlusion
Cohort B	LLI C7XR	100 fps (n=4)	20 mm/s	0.2 mm	Continuous flush through guiding catheter

LLI: Light Lab Imaging; fps: frames per second

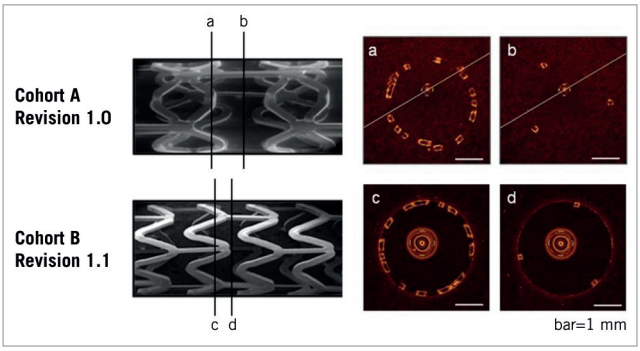

Figure 3. Scanning electro microscopy of the revision 1.0 and revision 1.1 BVS scaffolds, indicating the difference in strut arrangement from the out of phase zig-zag hoops in the revision 1.0 design, to the in-phase zig-zag hoops in the revision 1.1 design. The OCT images demonstrate the variation in the number of struts which can be seen along the length. The minimum number of struts seen in any one frame is three for both structures.

system), guide wire shadow (especially C7XR system) and so on. In view of this, the number of frames containing ≤3 struts was counted which represent the sections within the structure with the maximum unsupported arc.[2]

More importantly a three-dimensional assessment was also made by measuring the strut distribution longitudinally. This longitudinal assessment was accomplished by measuring the frequency of those frames containing the most visible number of struts along the entire length of the structure. In order to achieve this, we initially drew a graph which displayed the number of struts per frame as a function of the scaffold length (at 0.5 mm intervals along the length), (Figure 4). The graph showed that the number of struts per frame varied cyclically along the length of the scaffold. The number of observed crests was corrected for implant length.

The pullback images were reviewed on the LightLab Imaging (LLI) OCT imaging proprietary offline review workstation (LightLab Imaging Inc, Westford, MA, USA). The images were calibrated based on the reflection of the imaging catheter, which is the standard calibration technique for this system. OCT images were measured at 0.5 mm intervals, which take into account the frame rate, and the pullback speed which was 1.0 mm/s for the M2 system and 20 mm/s for the C7XR system. Thus in cases of 8.2 frames per second four frames interval were chosen; in cases of 15.6 fps eight frame intervals were chosen, and in cases of 100 fps three and two frame intervals were selected. OCT images were measured between the most proximal and distal frame that contained struts which were visible circumferentially. Stent areas were traced manually and the number of struts, each inter-strut angle, and the eccentricity of the OCT imaging catheter were analysed in each cross-sectional frame. The stent length was calculated as number of frames between the first and last frames divided by the frame rate. The number of analysed frames with struts, numbers of frames with struts ≤3, and the frames with an inter-strut angle >120º were all normalised for stent length. This was necessary because three Cohort A stents were 12 mm in length, whilst the remaining stent in Cohort A and all four Cohort B stents were 18 mm long.

Definitions

Inter-strut angle was defined as the angle created between two lines passing from the centre of gravity of the lumen, to the clockwise side of two consecutive struts (Figure 5). Eccentricity of the OCT imaging catheter was measured as illustrated in Figure 6. To assess inter-observer variability of the strut counts and inter-strut angle, two independent observers separately counted the number of struts on each frame.

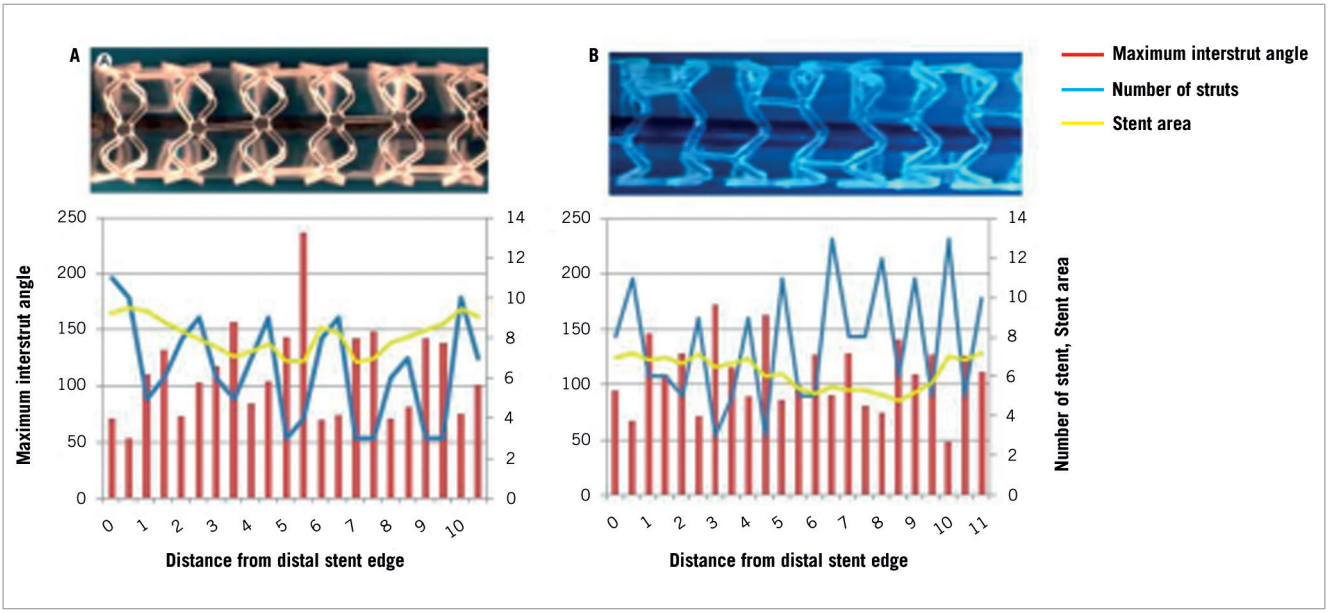

Figure 4. The cyclical variation in the maximum number of struts per frame along the structure's length. (A) revision 1.0 (cohort A) (B) revision 1.1, (cohort B).

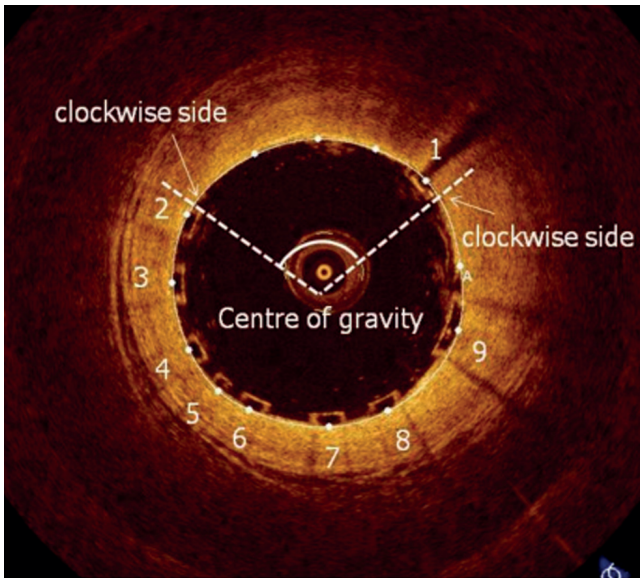

Figure 5. Inter-strut angle was defined as the angle created between two lines passing from the centre of gravity of the lumen, to the clockwise side of two consecutive struts.

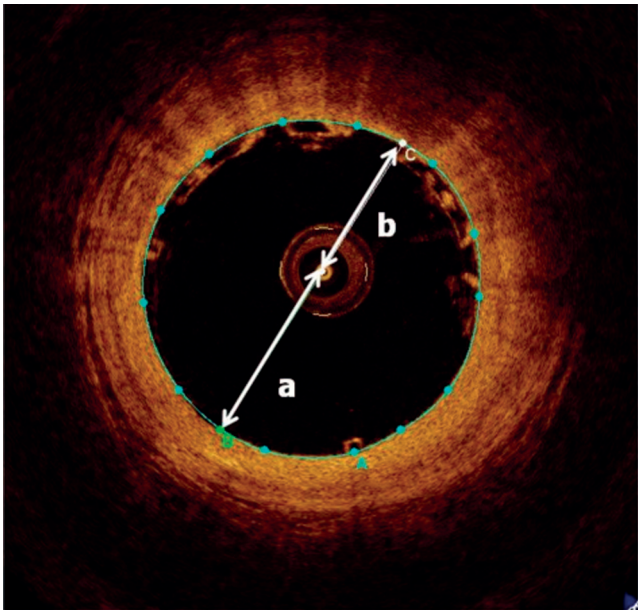

Figure 6. To assess eccentricity of the OCT catheter a diameter line was drawn which passed through the centre of the imaging catheter, and the lumen's centre of gravity. The centre of the imaging catheter was used to split this line into two parts, 'a' and 'b' as illustrated. The eccentricity of the imaging catheter was defined as the ratio between the two lines (b/a). A value of 1 indicated that the OCT catheter was central; other values indicated the catheter was eccentric.

Statistics

The current analysis is *ad hoc* and was not pre-specified in the protocol for either Cohort A or Cohort B of the ABSORB study. Discrete variables are presented as counts and percentages. Continuous variables are presented as means±SD. The inter-observer agreements for continuous variables are expressed through the inter-observer correlation coefficient for absolute agreement in a single measurement (IOC). On a frame-by-frame analysis the difference in the number of struts, the maximal inter-strut angle, and the inter-strut angle between ABSORB Cohorts A and B were compared using the t-test for independent samples. A two-sided p-value of less than 0.05 was considered statistically significant. All statistical analysis was performed using SPSS Version 14.0 (SPSS Inc., Chicago, IL, USA)

Results

A total of eight patients were included in the study, who were mostly male (62.5%), and had an age range from 46 to 76 years. The LAD was the most frequently imaged artery at 62.5%. The mean stent length was 13.5±3.5 mm and 18.0±0.0 mm for Cohort A and B respectively. The mean stent diameter was 3.0 mm for both groups. The results from the OCT analysis are presented on a patient level, and a frame-by-frame level in Table 2. The length of the implant was different between Cohort A and Cohort B, and therefore the number of struts was normalised for implant length. There were no significant differences in the number of struts normalised by length (p=0.78). There was no significant difference in the number of frames with ≤3 struts (p=0.96), or the number of frames containing an inter-strut angle of >120° (p=0.82). The mean maximum inter-strut angle was 152±8° and 152±19° for Cohort A and B respectively (p=0.98). On a frame-by-frame analysis, there were no significant difference in mean stent area, number of struts per frame, mean maximum inter-strut angle and mean inter-strut angle between both cohorts. Figure 4 demonstrates the cyclical variation in the maximum number of struts per frame, along the implant's length. There is a significantly higher number of crests per millimetre for Cohort B compared to Cohort A (0.51±0.12 vs. 0.71±0.05, p=0.041). The inter-observer correlation coefficient for strut count, maximum inter-strut angle, and inter-strut angle are reported in Table 3.

Table 2. Results of OCT analysis on a patient and frame-by-frame level for both groups.

	Cohort A	Cohort B	P Value
Patient (n)	4	4	
Analysed length (mm)	12.8±4.2	17.4±1.4	
Total No. of struts	754	1049	
No. of strut/mm	14.9±1.1	15.1±0.6	0.78
No. of frames (strut ≤3)/mm	0.2±0.2	0.2±0.1	0.96
Max inter-strut angle in pullback	152°±8	152°±19	0.98
No. of inter-strut angle (>120°)/mm	0.9±0.2	1.0±0.2	0.82
Analysed frame (n)	106	143	
Mean stent area (mm²)	7.9±1.1	8.0±1.5	0.72
No. of struts/frame	7.1±2.5	7.3±2.8	0.51
Average of max inter-strut angle	110.1°±40.4	107.6°±34.4	0.61
Mean inter-strut angle	59.1°±26.3	58.3°±28.7	0.83
Catheter eccentricity	0.3±0.2	0.5±0.2	<0.001

No.: number

Table 3. Results of frame-by-frame OCT analysis comparing results between two independent analysts.

	Observer 1	Observer 2	IOC
Strut counts			
Total no. frames	229	229	0.91
Total agreement (%)	99 (43.2)		
1 disagreement (%)	90 (39.3)		
>1 disagreement (%)	40 (17.5)		
Maximum angle			
Mean±SD (degree)	108°±37	112°±43	0.74
Absolute difference (degree)	14°±25		
Relative difference (%)	12±17		
Inter-strut angle			
Mean±SD (degree)	58°±28	60°±31	0.87
Absolute difference (degree)	8°±12		
Relative difference (%)	12±13		

IOC: inter-observer correlation coefficient (1=complete agreement between observers); SD: standard deviation; No.: number

Discussion

Due to its high resolution, OCT is an invaluable tool for the *in vivo* evaluation of coronary metallic stents. Recently the images obtained using OCT have been shown to be very useful in the assessment of the bioabsorption process of polymeric struts.[1,2] Both of these factors, together with the excellent reproducibility of OCT as demonstrated in this and previous studies,[6] indicate that it can be used reliably to study coronary stent geometry *in vivo*.

One of the major observations in the ABSORB Cohort A study was the alteration in the structure's geometry acutely and at follow-up, which may have been related to the number of struts along the implant's length.[2] This factor is best assessed by the measuring MCUSA, which unfortunately cannot be directly measured *in vivo,* but can be assessed by cross sectional and longitudinal strut distribution. In the present *ad hoc* analysis both structures had the same strut distribution when assessed in cross-section, but this was not the case longitudinally. On OCT frame-by-frame cross sectional analysis the number of struts and the inter-strut angle were the same for both designs. However the longitudinal distribution of the struts was different as indicated by the higher number of crests per millimetre for Cohort B compared to Cohort A. We propose that this increased frequency can be used as a surrogate marker of MCUSA, because when considering just this difference the Cohort B design has a lower MCUSA per unit length compared to the Cohort A design; a fact readily apparent from the two structures.

Historically acute and late recoil were responsible for the poorer clinical outcomes observed with balloon angioplasty. The introduction of stents addressed these problems by providing a permanent scaffold to minimise the effects of recoil. Haude et al compared the recoil in patients treated with balloon angioplasty and stenting with Palmaz-Schatz stents, and reported higher rates of acute recoil with balloon angioplasty with respect to vessel diameter (31% after balloon angioplasty vs. 3.5% after stenting) and area (48% after balloon angioplasty vs. 5.1% after stenting).[7] Similarly Painter et al reported late recoil with the Palmaz-Schatz stent at four month follow-up of only 0.6%.[8] These important observations are central to improved clinical outcomes observed with stenting when compared with balloon angioplasty.[9-11]

In recent times there have been safety concerns with permanent coronary stents,[12-15] and as a consequence interest has focused on the development of biodegradable stents. In principle, these implants are designed to provide enough radial force to provide a temporary scaffold preventing acute and late recoil, and then bioabsorb at a time when the vessel has fully healed and the concerns regarding vessel recoil have subsided.

Currently clinical studies of bioabsorbable stents have shown promising clinical outcomes.[1,2,16-20] Unfortunately results have also demonstrated that both bioabsorbable metallic and polymeric designs are yet to achieve the ideal balance between the maintenance of radial force, and the start of bioabsorption. The PROGRESS AMS study of the magnesium AMS-1 (absorbable metallic stent) stent demonstrated no deaths, myocardial infarctions or stent thrombosis at one year follow-up, however the rate of target lesion revascularisation was 45%. This was a result of vessel recoil of 42% which was attributable to the loss of radial force from the early and rapid degradation of the stent.[18,21] Similarly, in the ABSORB study of the polymeric BVS 1.0 design, there was no cardiac death, target vessel revascularisation or stent thrombosis during follow-up, however there was a reduction in stent area between baseline and six month follow-up. In an attempt to address these issues, significant modifications in stent design have been made. The initial AMS-1 stent[22] had degradation times as rapid as four weeks, whilst the new AMS-2 stent, with a different magnesium alloy, has an improved radial force, and a prolonged degradation time. The new Revision 1.1 BVS design is made of the same polymers, with processes modified to enable the scaffold to have and retain greater radial strength and scaffolding abilities for longer, and without changing the total absorption time.

Limitations

The study is limited by the small number of patients in each group, and the *ad hoc* nature of the analysis. Two different OCT technologies (time domain and frequency domain) were used in this study. Frequency domain enables a larger numbers of lines per cross-section and a wider range of field of view, therefore improving stent struts detection particularly in presence of an eccentric position of the OCT probe. We fully acknowledge that counting struts is subject to inter-observer variability.

Conclusion

This study has confirmed that the BVS Revision 1.1 scaffold has a different longitudinal strut distribution to that in Revision 1.0, indicating that the new design has a reduced MCUSA. These findings still need to be confirmed by a direct assessment of the MCUSA *in vivo* using for example, 3D-OCT (Figure 7).

In principle this reduction in MCUSA should reduce recoil; however the clinical implications of these design changes will only be apparent once the findings of the on-going ABSORB Cohort B study are reported.

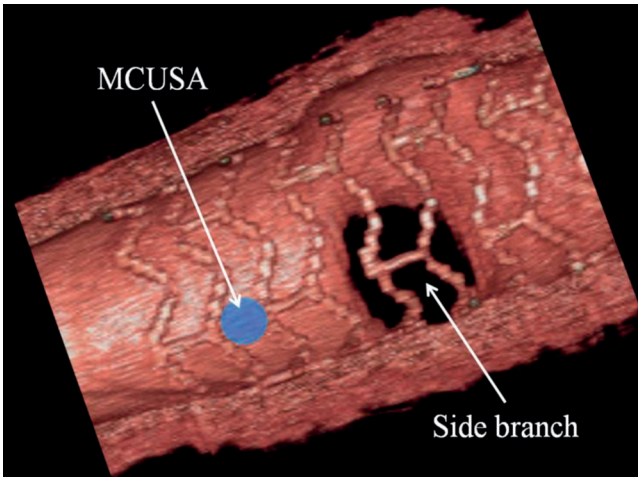

Figure 7. The direct in vivo assessment of maximum circular unsupported cross sectional area using 3D OCT. The strut arrangement across a side branch is also visualised.

References

1. Ormiston JA, Serruys PW, Regar E, Dudek D, Thuesen L, Webster MWI, Onuma Y, Garcia-Garcia HM, McGreevy R, Veldhof S. A bioabsorbable everolimus-eluting coronary stent system for patients with single de-novo coronary artery lesions (ABSORB): a prospective open-label trial. *Lancet* 2008;371:899-907.

2. Serruys PW, Ormiston JA, Onuma Y, Regar E, Gonzalo N, Garciaz-Garcia HM, Nieman K, Bruining N, Dorange C, Miquel-Hébert K, Veldhof S, Webster M, Thuesen L, Dudek D. A bioabsorbable everolimus-eluting coronary stent system (ABSORB): 2-year outcomes and results from multiple imaging methods. *Lancet* 2009;373:897-910.

3. Tanimoto S, Serruys PW, Thuesen L, Dudek D, de Bruyne B, Chevalier B, Ormiston JA. Comparison of in vivo acute stent recoil between the bioabsorbable everolimus-eluting coronary stent and the everolimus-eluting cobalt chromium coronary stent: insights from the ABSORB and SPIRIT trials. *Catheter Cardiovasc Interv* 2007;70:515-523.

4. Tanimoto S, Bruining N, van Domburg RT, Rotger D, Radeva P, Ligthart JM, Serruys PW. Late stent recoil of the bioabsorbable everolimus-eluting coronary stent and its relationship with plaque morphology. *J Am Coll Cardiol* 2008;52:1616-1620.

5. Ormiston JA, Serruys PW. Bioabsorbable Coronary Stents. *Circ Cardiovasc Intervent* 2009;2:255-260.

6. Gonzalo N, Garcia-Garcia HM, Serruys PW, Commissaris KH, Bezerra H, Gobbens P, Costa M, Regar E. Reproducibility of quantitative optical coherence tomography for stent analysis. *EuroIntervention* 2009;5:224-232.

7. Haude M, Erbel R, Issa H, Meyer J. Quantitative analysis of elastic recoil after balloon angioplasty and after intracoronary implantation of balloon-expandable Palmaz-Schatz stents. *J Am Coll Cardiol* 1993;21:26-34.

8. Painter JA, Mintz GS, Wong SC, Popma JJ, Pichard AD, Kent KM, Satler LF, Leon MB. Serial intravascular ultrasound studies fail to show evidence of chronic Palmaz-Schatz stent recoil. *Am J Cardiol* 1995;75:398-400.

9. Fischman DL, Leon MB, Baim DS, Schatz RA, Savage MP, Penn I, Detre K, Veltri L, Ricci D, Nobuyoshi M. A randomized comparison of coronary-stent placement and balloon angioplasty in the treatment of coronary artery disease. Stent Restenosis Study Investigators. *N Engl J Med* 1994;331:496-501.

10. Serruys PW, van Hout B, Bonnier H, Legrand V, Garcia E, Macaya C, Sousa E, van der Giessen W, Colombo A, Seabra-Gomes R, Kiemeneij F, Ruygrok P, Ormiston J, Emanuelsson H, Fajadet J, Haude M, Klugmann S, Morel MA. Randomised comparison of implantation of heparin-coated stents with balloon angioplasty in selected patients with coronary artery disease (Benestent II). *Lancet* 1998;352:673-681.

11. Serruys PW, de Jaegere P, Kiemeneij F, Macaya C, Rutsch W, Heyndrickx G, Emanuelsson H, Marco J, Legrand V, Materne P. A comparison of balloon-expandable-stent implantation with balloon angioplasty in patients with coronary artery disease. Benestent Study Group. *N Engl J Med* 1994;331:489-495.

12. Nordmann AJ, Briel M, Bucher HC. Mortality in randomized controlled trials comparing drug-eluting vs. bare metal stents in coronary artery disease: a meta-analysis. *Eur Heart J* 2006;27:2784-2814.

13. Lagerqvist B, James SK, Stenestrand U, Lindbäck J, Nilsson T, Wallentin L. Long-term outcomes with drug-eluting stents versus bare-metal stents in Sweden. *N Engl J Med* 2007;356:1009-1019.

14. Camenzind E, Steg PG, Wijns W. Stent thrombosis late after implantation of first-generation drug-eluting stents: a cause for concern. *Circulation* 2007;115:1440-1455; discussion 1455.

15. Wenaweser P, Daemen J, Zwahlen M, van Domburg R, Jüni P, Vaina S, Hellige G, Tsuchida K, Morger C, Boersma E, Kukreja N, Meier B, Serruys PW, Windecker S. Incidence and correlates of drug-eluting stent thrombosis in routine clinical practice. 4-year results from a large 2-institutional cohort study. *J Am Coll Cardiol* 2008;52:1134-1140.

16. Tamai H, Igaki K, Kyo E, Kosuga K, Kawashima A, Matsui S, Komori H, Tsuji T, Motohara S, Uehata H. Initial and 6-month results of biodegradable poly-l-lactic acid coronary stents in humans. *Circulation* 2000;102:399-404.

17. Tsuji T, Tamai H, Igaki K, Hsu YS, Kosuga K, Hata T, Okada M, Nakamura T, Fujita S. Four-year Follow-up of the Biodegradable Stent (IGAKI-TAMAI Stent). *Circ J* 2004;68:135.

18. Erbel R, Di Mario C, Bartunek J, Bonnier J, de Bruyne B, Eberli FR, Erne P, Haude M, Heublein B, Horrigan M, Ilsley C, Böse D, Koolen J, Lüscher TF, Weissman N, Waksman R. Temporary scaffolding of coronary arteries with bioabsorbable magnesium stents: a prospective, non-randomised multicentre trial. *Lancet* 2007;369:1869-1875.

19. Bosiers M, Deloose K, Verbist J, Peeters P. First clinical application of absorbable metal stents in the treatment of critical limb ischemia: 12-month results. *Vasc Dis Manag.* 2005;2:86-91.

20. Bosiers M, Peeters P, D'Archambeau O, Hendriks J, Pilger E, Düber C, Zeller T, Gussmann A, Lohle PNM, Minar E, Scheinert D, Hausegger K, Schulte K, Verbist J, Deloose K, Lammer J. AMS INSIGHT—absorbable metal stent implantation for treatment of below-the-knee critical limb ischemia: 6-month analysis. *Cardiovasc Intervent Radiol* 2009;32:424-435.

21. Waksman R, Erbel R, Di Mario C, Bartunek J, de Bruyne B, Eberli FR, Erne P, Haude M, Horrigan M, Ilsley C, Bose D, Bonnier H, Koolen J, Luscher TF, Weissman NJ, on behalf of the PROGRESS-AMS (Clinical Performance Angiographic Results of Coronary Stenting with Absorbable Metal Stents) Investigators. Early- and Long-Term Intravascular Ultrasound and Angiographic Findings After Bioabsorbable Magnesium Stent Implantation in Human Coronary Arteries. *J Am Coll Cardiol Intv* 2009;2:312-320.

22. Waksman R. Current state of the metallic bioabsorbable stent. EuroPCR 19th-22nd May 2009; Barcelona [online] Available www.europcronline.com/fo/lecture/view_slide.php?idCongres=5&id=7967. [Accessed 10th June 2009].